JACS
JOURNAL OF THE AMERICAN CHEMICAL SOCIETY
Communication
pubs.acs.org/JACS

Broadband Emission in Two-Dimensional Hybrid Perovskites: The Role of Structural Deformation

Daniele Cortecchia,[†,‡] Stefanie Neutzner,[‡] Ajay Ram Srimath Kandada,[‡] Edoardo Mosconi,[§,∥] Daniele Meggiolaro,[§,∥] Filippo De Angelis,[*,§,∥] Cesare Soci,[⊥] and Annamaria Petrozza[*,‡]

[†]Interdisciplinary Graduate School, Energy Research Institute @ NTU(ERI@N), Nanyang Technological University, 639798 Singapore

[‡]Centre for Nano Science and Technology (CNST@PoliMi), Istituto Italiano di Tecnologia, via Pascoli 70/3, Milan 20133, Italy

[§]Istituto CNR di Scienze e Tecnologie Molecolari, c/o Dipartimento di Chimica, Università di Perugia, Perugia I-06123, Italy

[∥]CompuNet, Istituto Italiano di Tecnologia, Via Morego 30, 16163 Genova, Italy

[⊥]Division of Physics and Applied Physics, School of Physical and Mathematical Sciences, Nanyang Technological University, 637371 Singapore

Supporting Information

ABSTRACT: Only a selected group of two-dimensional (2D) lead−halide perovskites shows a peculiar broad-band photoluminescence. Here we show that the structural distortions of the perovskite lattice can determine the defectivity of the material by modulating the defect formation energies. By selecting and comparing two archetype systems, namely, $(NBT)_2PbI_4$ and $(EDBE)PbI_4$ perovskites (NBT = *n*-butylammonium and EDBE = 2,2-(ethylenedioxy)bis(ethylammonium)), we find that only the latter, subject to larger deformation of the Pb−X bond length and X−Pb−X bond angles, sees the formation of V_F color centers whose radiative decay ultimately leads to broadened PL. These findings highlight the importance of structural engineering to control the optoelectronic properties of this class of soft materials.

Hybrid perovskites provide the unique opportunity of tuning the dimensionality of the electronic landscape by controlling the nature of the organic cation.[1] 3D perovskites have been successfully employed in photovoltaic and light-emitting devices,[2,3] and 2D perovskites have recently been explored.[4−6] These consist of alternating organic and inorganic layers, with charge carriers confined within the inorganic network, similar to a multiquantum well structure. This leads to a large exciton binding energy (EBE) up to 300 meV,[1] compared to that of 3D perovskites where EBE is less than 50 meV.[7] Therefore, 2D perovskites usually show extremely narrow-band photoluminescence (PL) spectra, typically from free-excitonic states, holding a great promise in advanced optoelectronic applications such as lasing and polariton devices.[8,9] A subclass of 2D perovskites however has recently attracted attention for their potential application in broadband solid-state lighting due to the presence of highly Stokes-shifted light emission with full width at half-maximum (fwhm) up to 600−700 meV.[10]

Such broadband emission was observed irrespective of the crystal orientation and with no evident correlation with the chemical composition.[10−13] Recently, its appearance in Cl- and Br-based perovskites was ascribed to charge self-trapping phenomena.[14−16] However, the reason why self-localization is favored only in certain perovskites, in competition with sharp free-excitonic emission, is yet to be clarified. Structural deformations in traditional inorganic perovskites are known to play fundamental roles in ferro- and piezo-electricity and superconductivity.[17] Despite molecular rotations and octahedral distortions being considered in theoretical works on 3D perovskites,[18] their influence on luminescence properties has not yet been investigated. Here, we show that structural distortions of the inorganic lattice play a key role in carrier localization and the subsequent broadband emission.

Synthetic chemistry offers powerful tools to control the perovskite structural properties. Here we synthesize, *ad hoc*, two representative 2D perovskites, $(NBT)_2PbI_4$ and $(EDBE)PbI_4$ (Figure 1a,b), having the same inorganic network (PbI_4^{2-})

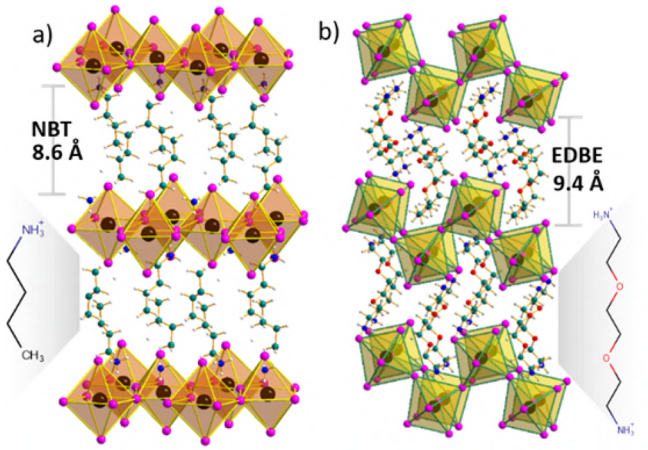

Figure 1. Crystal structures of (a) $(NBT)_2PbI_4$[19] and (b) $(EDBE)PbI_4$,[10] with their templating cations: NBT = *n*-butylammonium and EDBE = 2,2-(ethylenedioxy)bis(ethylammonium).

Received: October 8, 2016
Published: December 26, 2016

DOI: 10.1021/jacs.6b10390
J. Am. Chem. Soc. 2017, 139, 39−42

but assembling in distinct crystalline configurations. This is achieved by exploiting the templating mono- and ditopic organic cations NBT = *n*-butylammonium and EDBE = 2,2-(ethylenedioxy)bis(ethylammonium) (Figure 1a,b). These two linkers direct the crystal growth along different perovskite cuts, resulting in the flat <100>-oriented $(NBT)_2PbI_4$ and rippled $(EDBE)PbI_4$, characterized by the <110>-oriented zigzag structure.[10,19] These were reported to crystallize with orthorhombic and monoclinic crystal systems, respectively,[10,19] in agreement with our thin film X-ray diffraction measurements (Figure S1).

To investigate the effect of such a structural difference, we performed Raman measurements on perovskite crystals (Figure 2), films (Figure S2), and iodide salts of their organic

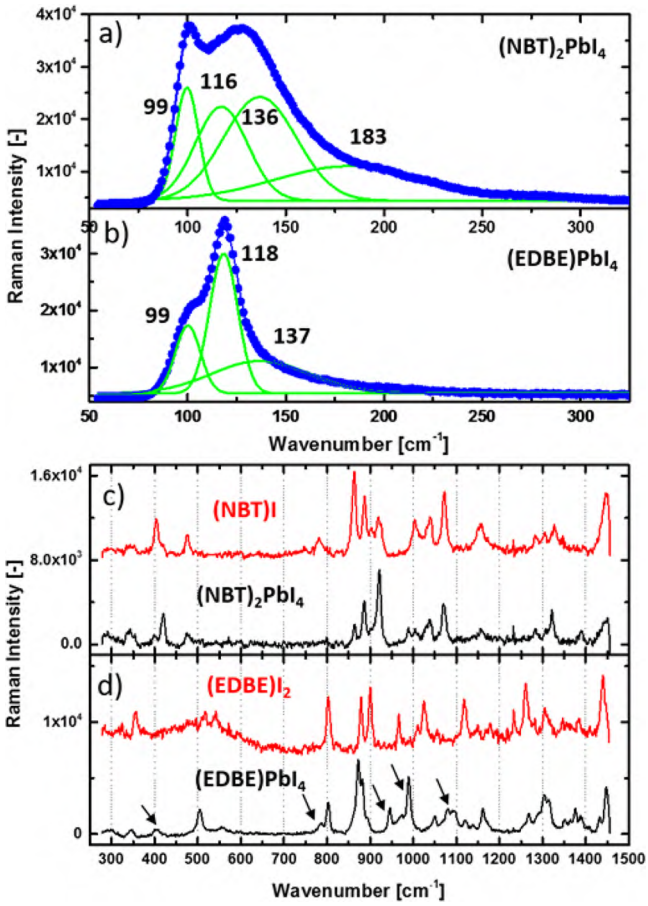

Figure 2. Raman spectra of (a, c) $(NBT)_2PbI_4$ and (b, d) $(EDBE)PbI_4$. (c, d) Active modes of the pure iodide salts (red) and those of the organic cation after formation of the perovskite (black). The black arrows indicate new active modes of $EDBE^{2+}$ upon perovskite formation.

precursors. Similar to the Raman spectrum of $MAPbI_3$ (MA = methylammonium), four bands appear between 80 and 300 cm^{-1} (Figures 2a,b).[20] Following previous assignments,[20−23] we attribute the band at 99 cm^{-1} to the Pb−I stretching mode. The remaining three bands are assigned to vibrational modes of the ammonium moieties coupled with the inorganic part. The signals at 116−118 and 136 cm^{-1} are ascribed to libration modes, and the band at 183 cm^{-1} is ascribed to torsional modes.[20,22] While the peak at 99 cm^{-1} is prominent in the Raman spectrum of $(NBT)_2PbI_4$, resembling that of $MAPbI_3$, it is partially deactivated in $(EDBE)PbI_4$; such weakening of the Pb−I intensity mode results from the increased angular distortion of the latter (Table S1 and S2). Moreover, the band at 183 cm^{-1} is absent in $(EDBE)PbI_4$, and the strength of the 136 cm^{-1} mode is significantly reduced. This observation can be interpreted as a higher degree of conformational constraint of the ammonium moieties in the <110>-oriented perovskite, due to their strong interaction with the enclosing inorganic lattice.[24]

We also compare the Raman spectra of the organic cation (between 300 and 1500 cm^{-1}) within the perovskite lattice and the pristine molecules (Figure 2c,d). Here, the spectral features belong to pure vibrational modes of the organic part.[21,25] (NBT)I preserves all its active modes when embedded in the perovskite with only small changes in the relative intensities of the peaks (Figure 2c). On the contrary, new modes appear in $(EDBE)I_2$ when cocrystallized with PbI_2 (black arrows in Figure 2d). We argue that $EDBE^{2+}$ in the perovskite is forced into a different conformation due to its greater interaction with the inorganic cage, mutually affecting the distortion of the Pb−I framework.

The consequences of such structural transformation on the optical properties are important. The absorption and PL spectra of polycrystalline films (Figure S3) are shown in Figure 3a,b.

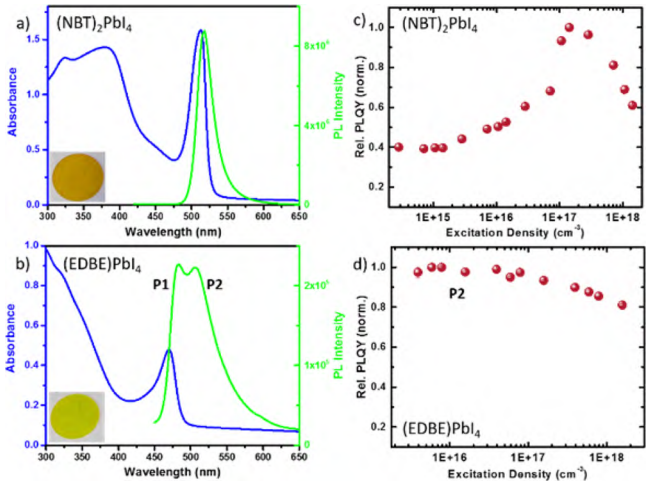

Figure 3. Steady-state absorption (blue) and photoluminescence (green) of (a) $(NBT)_2PbI_4$ and (b) $(EDBE)PbI_4$. The insets show the structure induced color change (from orange to yellow). Relative photoluminescence quantum yield (PLQY) against excitation density for (c) $(NBT)_2PbI_4$ and (d) $(EDBE)PbI_4$.

The optical band-edge of $(EDBE)PbI_4$ is blue-shifted by 44 nm with respect to $(NBT)_2PbI_4$ with excitonic resonances at 469 and 513 nm, respectively (Figure 3). This drastic change in band gap is a fingerprint of the different structural arrangement of the inorganic framework in the <100>- and <110>-oriented perovskites.

$(NBT)_2PbI_4$ shows narrow-band emission (FWHM = 25 nm) at 517 nm with Stokes shift of just 4 nm, while $(EDBE)PbI_4$ exhibits much broader PL (fwhm = 70 nm) comprising a narrow-band bandgap emission peaked at 483 nm (P1) overlapped with a broader, red-shifted band at 507 nm (P2). P1 and P2 can be distinguished in thinner films, while thicker ones predominantly show a featureless broadband attributable to losses due to reabsorption (Figure S4). Both the materials have absolute photoluminescence quantum yield (PLQY) below 1%, with $(NBT)_2PbI_4$ being more emissive than

DOI: 10.1021/jacs.6b10390
J. Am. Chem. Soc. 2017, 139, 39−42

(EDBE)PbI_4. To obtain reliable intensity dependent trends, it is essential to perform measurements on thicker samples, where it is not possible to clearly observe P1 in (EDBE)PbI_4 (Figure S4). Thus, the trend of only P2 is reported in Figure 3. In $(NBT)_2PbI_4$, the relative PLQY of the band-to-band emission enhances with excitation density, with a drop at high excitations due to Auger recombination (Figures 3c and S5). On the contrary, P2 in (EDBE)PbI_4 shows a monotonic reduction, suggesting its origin from electronic states whose occupation probability reduces at higher excitation densities (Figures 3d and S5). An identical trend is observed in single crystals (Figure S6). Such behavior is reminiscent of PL from intragap defect states, saturated at higher densities. Presence of radiative defects within the perovskite lattice was also reported in 3D perovskites.[26−29] This implies that (EDBE)PbI_4 contains a higher density of radiative color centers.

To ascertain the structure−PL properties relationship, we determined the degree of structural strain of the perovskite considering the distortions of the inorganic building blocks, the octahedra PbX_6. The deformation of O_h symmetry involves modifications in Pb−X bond length (d) and X−Pb−X angles (α), with changes in edge length (X−X distances) and O_h volume (V) compared to that of the ideal structure.[30] Robinson et al.[31] developed a quantitative evaluation of these parameters introducing the octahedral elongation λ_{oct} and octahedral angle variance σ^2_{oct}:

$$\lambda_{oct} = \frac{1}{6}\sum_{i=1}^{6}(d_i/d_0)^2 \quad (1)$$

$$\sigma^2_{oct} = \frac{1}{11}\sum_{i=1}^{12}(\alpha_i - 90)^2 \quad (2)$$

where d_i are the Pb−X bond lengths, d_0 is the center-to-vertex distance of a regular polyhedron of the same volume, and α_i are the X−Pb−X angles. PL broadening follows the increased structural distortion of (EDBE)PbI_4 (λ_{oct} = 1.0058; σ^2_{oct} = 14.2) compared to that of $(NBT)_2PbI_4$ (λ_{oct} = 1.0016; σ^2_{oct} = 5.6). This observation is corroborated by evaluating the structural parameters of broadband emitting perovskites compared to those of typical narrowband emitters (Tables S1 and S2). By plotting λ_{oct} against σ^2_{oct}, it appears that higher distortion factors closely correlate with PL broadening (Figure S7).

To rationalize the structural effects on the defectivity and energetic landscape, we performed *ab initio* calculations on perfect and defective crystals, considering iodine interstitials and vacancies (I_i, V_I) and lead vacancies (V_{Pb}) (Figure S8 and Table S3).[32] We find two different structures for the neutral Pb vacancy: (i) a relaxed structure where a vicinal iodine moves to the V_{Pb} site to form an I_3^- trimer (Figure 4a) and (ii) a structure with V_{Pb} remaining in the position where the lead was removed (Figure 4b), similar to the stable structure found for the 2- and 1-charge states.[33,34] The stability of the two structures depends on the material: While these are isoenergetic in $(NBT)PbI_4$, I_3^- formation is strongly favored in (EDBE)PbI_4 by ∼1 eV. The relaxed structure corresponds to the oxidation of two iodides by two holes left in the defect site upon neutral V_{Pb} formation. In (EDBE)PbI_4, the formation of I_3^- is driven by undercoordinated iodine atoms at the organic/inorganic interface, only partly charge stabilized by $EDBE^{2+}$, and can thus lead to large lattice rearrangements. In $(NBT)_2PbI_4$, there is one frontier iodine atom per organic cation (two such iodine atoms are instead present in (EDBE)PbI_4) with a consequently stronger electrostatic interaction that disfavors the vicinal iodine motion from forming I_3^-. Similar point defects, consisting in a V-center coupled to an adjacent cation vacancy, were demonstrated in LiF: These are known as V_F centers and regarded as "the antimorph of the F centers", involving the complementary electron trapping at a halogen vacancy.[35,36]

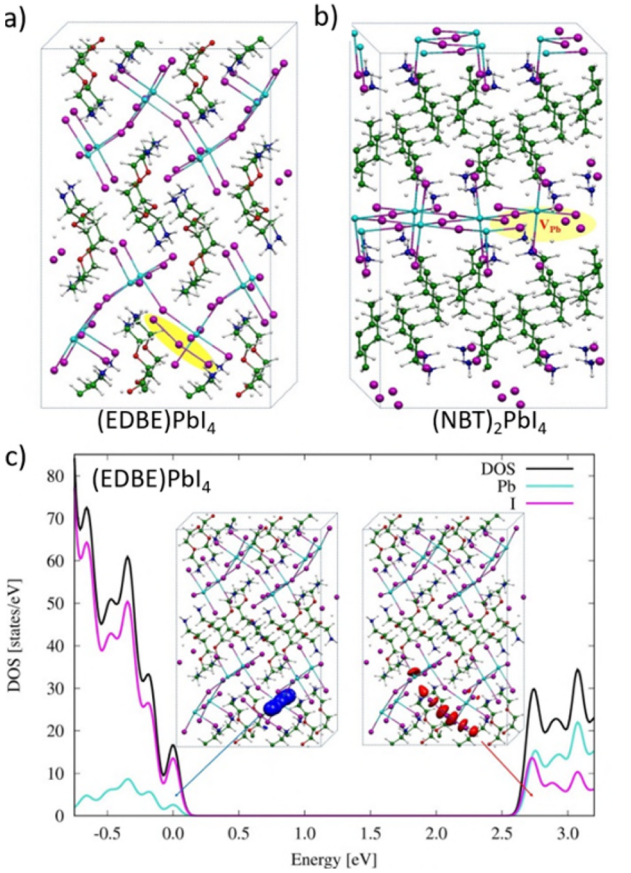

Figure 4. Geometry structures of neutral vacancy of (a) (EDBE)PbI_4 and (b) $(NBT)_2PbI_4$. (c) DOS of the neutral lead vacancy (EDBE)PbI_4 and the relative isodensity plot of the defect states.

Quantitative estimation of the electronic structure is achieved with hybrid DFT calculations including spin−orbit coupling (PBE0-SOC).[34] For the pristine (EDBE)PbI_4, we calculate a band gap of 2.83 eV, excellently matching the experimental excitonic peak (2.64 eV), considering the typical EBE of 2D perovskites (200−300 meV). The introduction of neutral V_{Pb} generates two electronic states in the DOS (one occupied, one unoccupied) at 0.16 and 0.05 eV above and below the valence and conduction band edges (Figure 4c). The calculated optical absorption spectrum of the defective system, using the random phase approximation neglecting nonlocal fields effects (Figure S9), highlights the presence of an optical transition at 0.21 eV below the main band gap absorption peak. This corresponds to the HOMO−LUMO transition of I_3^-, with intensity of $\sim^1/_4$ the cross section of the band gap transition. Therefore, we associate the emergence of these states with the emissive traps leading to Stokes-shifted, broadened luminescence according to the relaxation mechanism typical of trapped charge carriers.[13,14] Our analysis highlights the crucial role of the templating cation to assist charge localization, indicating that increased structural distortions in the PbX_6 octahedral coordination of (EDBE)PbI_4

DOI: 10.1021/jacs.6b10390
J. Am. Chem. Soc. 2017, 139, 39−42

lower the energy barrier for hole self-trapping and stabilize the formation of I_3^-. Ultimately, this finding may have relevance also in 3D perovskites, where octahedral distortions may be finely tuned by the cation enclosed in the cubooctahedral cavities to modifying the tendency to undergo charge trapping. Further work is to be conducted in this direction.

In summary, we showed that geometrical distortions of the perovskite lattice closely affect its defectivity and corresponding charge relaxation dynamics, exemplified by the evidence of V_F centers formation in (EDBE)PbI_4. Our findings stress the importance of structural engineering in hybrid perovskites to achieve full control over the material properties, with high relevance for photovoltaic and light emission applications.

■ ASSOCIATED CONTENT

Supporting Information

The Supporting Information is available free of charge on the ACS Publications website at DOI: 10.1021/jacs.6b10390.

Experimental and computational details; perovskite distortion parameters (PDF)

■ AUTHOR INFORMATION

Corresponding Authors

*Annamaria.Petrozza@iit.it
*filippo@thch.unipg.it

ORCID

Annamaria Petrozza: 0000-0001-6914-4537

Notes

The authors declare no competing financial interest.

■ ACKNOWLEDGMENTS

We acknowledge the European seventh framework program under grant agreement no. 604032 of the MESO project, EU Horizon 2020 Research and Innovation Program under grant agreement no. 643238 (SYNCHRONICS), the Ministry of Education (MOE2013-T2-044), the National Research Foundation (NRF-CRP14-2014-03) of Singapore, and the project PERSEO-"PERrovskite-based Solar cells: towards high Efficiency and long-term stability" (Bando PRIN 2015-Italian Ministry of University and Scientific Research (MIUR) Decreto Direttoriale November 4, 2015 n. 2488, project number 20155LECAJ) and CARIPLO foundation (IPER-LUCE No. 2015-0080) for funding.

■ REFERENCES

(1) Saparov, B.; Mitzi, D. B. *Chem. Rev.* **2016**, *116*, 4558.
(2) Cho, H.; Jeong, S.-H.; Park, M.-H.; Kim, Y.-H.; Wolf, C.; Lee, C.-L.; Heo, J. H.; Sadhanala, A.; Myoung, N.; Yoo, S.; Im, S. H.; Friend, R. H.; Lee, T.-W. *Science* **2015**, *350*, 1222.
(3) Kim, Y.-H.; Cho, H.; Lee, T.-W. *Proc. Natl. Acad. Sci. U. S. A.* **2016**, *113*, 11694.
(4) Tsai, H.; Nie, W.; Blancon, J.-C.; Stoumpos, C. C.; Asadpour, R.; Harutyunyan, B.; Neukirch, A. J.; Verduzco, R.; Crochet, J. J.; Tretiak, S.; Pedesseau, L.; Even, J.; Alam, M. A.; Gupta, G.; Lou, J.; Ajayan, P. M.; Bedzyk, M. J.; Kanatzidis, M. G.; Mohite, A. D. *Nature* **2016**, *536*, 312.
(5) Yuan, M.; Quan, L. N.; Comin, R.; Walters, G.; Sabatini, R.; Voznyy, O.; Hoogland, S.; Zhao, Y.; Beauregard, E. M.; Kanjanaboos, P.; Lu, Z.; Kim, D. H.; Sargent, E. H. *Nat. Nanotechnol.* **2016**, *11*, 872.
(6) Byun, J.; Cho, H.; Wolf, C.; Jang, M.; Sadhanala, A.; Friend, R. H.; Yang, H.; Lee, T.-W. *Adv. Mater.* **2016**, *28*, 7515.
(7) Galkowski, K.; Mitioglu, A.; Miyata, A.; Plochocka, P.; Portugall, O.; Eperon, G. E.; Wang, J. T.-W.; Stergiopoulos, T.; Stranks, S. D.; Snaith, H. J.; Nicholas, R. J. *Energy Environ. Sci.* **2016**, *9*, 962.
(8) Lanty, G.; Zhang, S.; Lauret, J. S.; Deleporte, E.; Audebert, P.; Bouchoule, S.; Lafosse, X.; Zuñiga-Pérez, J.; Semond, F.; Lagarde, D.; Médard, F.; Leymarie, J. *Phys. Rev. B: Condens. Matter Mater. Phys.* **2011**, *84*, 195449.
(9) Deschler, F.; Price, M.; Pathak, S.; Klintberg, L. E.; Jarausch, D.-D.; Higler, R.; Hüttner, S.; Leijtens, T.; Stranks, S. D.; Snaith, H. J.; Atatüre, M.; Phillips, R. T.; Friend, R. H. *J. Phys. Chem. Lett.* **2014**, *5*, 1421.
(10) Dohner, E. R.; Jaffe, A.; Bradshaw, L. R.; Karunadasa, H. I. *J. Am. Chem. Soc.* **2014**, *136*, 13154.
(11) Dohner, E. R.; Hoke, E. T.; Karunadasa, H. I. *J. Am. Chem. Soc.* **2014**, *136*, 1718.
(12) Li, Y. Y.; Lin, C. K.; Zheng, G. L.; Cheng, Z. Y.; You, H.; Wang, W. D.; Lin, J. *Chem. Mater.* **2006**, *18*, 3463.
(13) Yangui, A.; Garrot, D.; Lauret, J. S.; Lusson, A.; Bouchez, G.; Deleporte, E.; Pillet, S.; Bendeif, E. E.; Castro, M.; Triki, S.; Abid, Y.; Boukheddaden, K. *J. Phys. Chem. C* **2015**, *119*, 23638.
(14) Hu, T.; Smith, M. D.; Dohner, E. R.; Sher, M.-J.; Wu, X.; Trinh, M. T.; Fisher, A.; Corbett, J.; Zhu, X. Y.; Karunadasa, H. I.; Lindenberg, A. M. *J. Phys. Chem. Lett.* **2016**, *7*, 2258.
(15) Cortecchia, D.; Yin, J.; Bruno, A.; Lo, S.-Z. A.; Gurzadyan, G. G.; Mhaisalkar, S. G.; Brèdas, J.-L.; Soci, C. 2016, arXiv:1603.01284v2. arXiv.org e-Print archive. https://arxiv.org/abs/1603.01284 (accessed October 3, 2016).
(16) Pelant, I.; Valenta, J. *Luminescence Spectroscopy of Semiconductors*; OUP: Oxford, 2012.
(17) Herklotz, A.; Wong, A. T.; Meyer, T.; Biegalski, M. D.; Lee, H. N.; Ward, T. Z. *Sci. Rep.* **2016**, *6*, 26491.
(18) Egger, D. A.; Rappe, A. M.; Kronik, L. *Acc. Chem. Res.* **2016**, *49*, 573.
(19) Billing, D. G.; Lemmerer, A. *Acta Crystallogr., Sect. B: Struct. Sci.* **2007**, *63*, 735.
(20) Quarti, C.; Grancini, G.; Mosconi, E.; Bruno, P.; Ball, J. M.; Lee, M. M.; Snaith, H. J.; Petrozza, A.; Angelis, F. D. *J. Phys. Chem. Lett.* **2014**, *5*, 279.
(21) Brivio, F.; Frost, J. M.; Skelton, J. M.; Jackson, A. J.; Weber, O. J.; Weller, M. T.; Goñi, A. R.; Leguy, A. M. A.; Barnes, P. R. F.; Walsh, A. *Phys. Rev. B: Condens. Matter Mater. Phys.* **2015**, *92*, 144308.
(22) Gottesman, R.; Gouda, L.; Kalanoor, B. S.; Haltzi, E.; Tirosh, S.; Rosh-Hodesh, E.; Tischler, Y.; Zaban, A.; Quarti, C.; Mosconi, E.; De Angelis, F. *J. Phys. Chem. Lett.* **2015**, *6*, 2332.
(23) Pérez-Osorio, M. A.; Milot, R. L.; Filip, M. R.; Patel, J. B.; Herz, L. M.; Johnston, M. B.; Giustino, F. *J. Phys. Chem. C* **2015**, *119*, 25703.
(24) Ivanovska, T.; Quarti, C.; Grancini, G.; Petrozza, A.; De Angelis, F.; Milani, A.; Ruani, G. *ChemSusChem* **2016**, *9*, 2994.
(25) Teixeira-Dias, J. J. C.; de Carvalho, L. A. E. B.; da Costa, A. M. A.; Lampreia, I. M. S.; Barbosa, E. F. G. *Spectrochimica Acta Part A: Molecular Spectroscopy* **1986**, *42*, 589.
(26) Motti, S. G.; Gandini, M.; Barker, A. J.; Ball, J. M.; Srimath Kandada, A. R.; Petrozza, A. *ACS Energy Letters* **2016**, *1*, 726.
(27) Kong, W.; Ye, Z.; Qi, Z.; Zhang, B.; Wang, M.; Rahimi-Iman, A.; Wu, H. *Phys. Chem. Chem. Phys.* **2015**, *17*, 16405.
(28) Neutzner, S.; Srimath Kandada, A. R.; Lanzani, G.; Petrozza, A. *J. Mater. Chem. C* **2016**, *4*, 4630.
(29) Wehrenfennig, C.; Liu, M.; Snaith, H. J.; Johnston, M. B.; Herz, L. M. *APL Mater.* **2014**, *2*, 081513.
(30) Thomas, N. *Acta Crystallogr., Sect. B: Struct. Sci.* **1989**, *45*, 337.
(31) Robinson, K.; Gibbs, G. V.; Ribbe, P. H. *Science* **1971**, *172*, 567.
(32) Mosconi, E.; Meggiolaro, D.; Snaith, H. J.; Stranks, S. D.; De Angelis, F. *Energy Environ. Sci.* **2016**, *9*, 3180.
(33) Azpiroz, J. M.; Mosconi, E.; Bisquert, J.; De Angelis, F. *Energy Environ. Sci.* **2015**, *8*, 2118.
(34) Du, M.-H. *J. Phys. Chem. Lett.* **2015**, *6*, 1461.
(35) Känzig, W. *J. Phys. Chem. Solids* **1960**, *17*, 80.
(36) Kao, C.-t.; Rowan, L. G.; Slifkin, L. M. *Phys. Rev. B: Condens. Matter Mater. Phys.* **1990**, *42*, 3142.

DOI: 10.1021/jacs.6b10390
J. Am. Chem. Soc. 2017, 139, 39−42